HAIT Journal of Science and Engineering, Volume 1, Issue 1, pp. 130-151

Infrared absorption in quantum crossbars *

Igor Kuzmenko and Sergey Gredeskul *

Department of Physics, Ben-Gurion University of the Negev,
Beer-Sheva 84105, Israel
* *Corresponding author: sergeyg@bgumail.bgu.ac.il*
Received 1 December 2003

Abstract

Double quantum crossbars (QCB) is a superlattice formed by two crossed interacting arrays of metallic nanotubes or quantum wires. The system possesses the Luttinger liquid (LL) fixed point, and a rich Bose-type excitation spectrum (plasmon modes). QCB plasmons may be involved in resonance diffraction of incident electromagnetic waves and in optical absorption in the infrared (IR) part of the spectrum. The absorption of external electric field in QCB strongly depends on the direction of the wave vector of an incident wave. As a result two types of $1D \rightarrow 2D$ dimensional crossover with varying angle of an incident wave or its frequency can be observed.

PACS: 78.67.-n; 77.22.Gm; 73.90.+f

1 Introduction

QCB is a double $2D$ grid formed by two superimposed crossing arrays of parallel conducting quantum wires [1 - 4], molecular chains [5] or single wall carbon nanotubes (SWCNT) [4, 6 - 8]. It represents a novel artificial nano-object which is one of the most attractive architectures for designing molecular-electronic circuits for computational application [5, 6, 9]. Similar structures with the same crossbar geometry also arise naturally as, e.g., crossed striped phases of doped transition metal oxides [10]. The possibility

*Presented at Russian-Israeli Conference *Frontiers in Condensed Matter Physics.* Shoresh, Israel, 19-24 October 2003

of excitation of one of the QCB constituents (nanotube, a single wire) by external electric field and existence of bistable conformations of other of them (molecular chain [11]) together with mechanical flexibility makes QCB an excellent candidate for an element of random access memory for molecular computing.

From a topological point of view, QCB is in a sense an object with intermediate dimensionality. Its spectral properties can not be treated in terms of purely 1D or $2D$ electron liquid theory. A constituent element of QCB (quantum wire or nanotube) possesses the Luttinger liquid (LL) like spectrum [12, 13]. A single array of parallel quantum wires is still a LL-like system qualified as a sliding phase [7] provided the pure electrostatic interaction between adjacent wires is taken into account. If an inter-wire tunneling is possible, the electronic spectrum of an array is that of $2D$ Fermi liquid (FL) [14, 15].

Similar low-energy, long-wave properties are characteristic of QCB as well. Its phase diagram inherits some properties of a sliding phases in case when the wires and arrays are coupled only by capacitive interaction [7, 16]. When inter-array electron tunneling is possible, say, in crosses, dimensional crossover from LL to $2D$ FL occurs [7, 17, 18]. If tunneling is suppressed and the two arrays are coupled only by electrostatic interaction in the crosses, the system possesses the LL zero energy fixed point, and a rich Bose-type excitation spectrum (plasmon modes) arises at finite energies in $2D$ Brillouin zone (BZ) [16, 19]. These QCB plasmons can be treated as a set of dipoles distributed within QCB constituents. In a single wire the density of the dipole momenta is proportional to the LL boson field $\theta(x)$ (x is the coordinate along the wire).

Two sets of coupled $1D$ dipoles form unique system which possesses the properties of $1D$ or $2D$ liquid depending on the type of experimental probe. Some possibilities of observing $1D \to 2D$ crossover in transport measurements (which give information about the nearest vicinity of the LL fixed point at $(q, \omega, T) \to 0$) were discussed in Ref. [7]. Later on, other crossover effects such as appearance of non-zero transverse space correlators and periodic energy transfer between arrays ("Rabi oscillations") were studied [20, 19, 21]. Observation of these effects probes the QCB spectral properties well beyond the sliding phase region.

However, the direct manifestation of crossover is the response to an external ac electromagnetic field. To estimate this response, one should note that the two main parameters characterizing the plasmon spectrum in QCB are the Fermi velocity v of electrons in a wire and the QCB period a (we assume both periods to be equal). These parameters define both the typ-

ical QCB plasmon wave numbers $q = |\mathbf{q}| \sim Q = 2\pi/a$ and the typical plasmon frequencies $\omega \sim \omega_Q = vQ$. Choosing according to Refs. [13, 6] $v \approx 8 \cdot 10^7$ cm/sec and $a \approx 20$ nm, one finds that the characteristic plasmon frequencies lie in the far IR region $\omega \sim 10^{14}$ sec^{-1}, while the characteristic wave vectors are estimated as $q \sim 10^6 cm^{-1}$.

In this paper we study the possibilities of direct observation of dimensional crossover at finite frequencies and wave vectors (i.e. outside the LL fixed point) by the methods of IR spectroscopy. We show that these methods provide an effective tool for investigating the plasmon spectra in wide enough (q, ω) region. They allow scanning of the $2D$ Brillouin zone in various directions and thereby elucidate dimensional crossover in high symmetry points of the BZ.

Let us consider a double square QCB interacting with an external infrared radiation (generalization to more complicated geometries is straightforward). The plasmon velocity v is much smaller than the light velocity c and the light wave vector k is three orders of magnitude smaller than the characteristic plasmon wave vector Q corresponding to the same frequency. Therefore, an infrared radiation incident directly on an *isolated* array, can excite plasmon only with $\omega = 0$, or in other words it cannot excite plasmons at all. However in QCB geometry, each array serves as a diffraction lattice for its partner, giving rise to Umklapp processes of wave vectors nQ, n integer. As a result, excitation of plasmons in the BZ center $q = 0$ with frequencies $\omega = nvQ$ occurs.

To excite QCB plasmons with $q \neq 0$ one may use an additional diffraction lattice (DL) with period $A > a$ coplanar with the QCB. Here the diffraction field contains space harmonics with wave vectors $2\pi M/A$, M integer, that enables one to scan plasmon spectrum within the BZ. Dimensional crossover manifests itself in the appearance of additional absorption lines when the wave vector of the diffraction field is oriented along specific directions. In the general case one observes single absorption lines forming two sets of equidistant series. On the other hand, an equidistant series of split doublets can be observed in the main resonance direction (QCB diagonal). In the case of higher resonance directions, absorption lines form an alternating series of singlets and split doublets demonstrating new type of dimensional crossover related to the frequency change with direction fixed.

The structure of the paper is as follows. In Section 2, we briefly describe double square QCB and its spectral properties. Interaction of QCB with external electric field is studied in Section 3. In its first part we consider the case when the incident infrared radiation falls directly on the QCB (Subsection 3.1). The second part 3.2 is devoted to possible scanning of QCB

spectrum with the help of an external DL. In the Conclusion we summarize the results obtained.

2 Double square QCB

A square QCB is a $2D$ grid, formed by two periodically crossed perpendicular arrays of $1D$ quantum wires or carbon nanotubes. Arrays are labelled by indices $j = 1(2)$ and the wires within the first (second) array are labelled by an integer index n_2 (n_1). In experimentally realizable setups, QCB is a cross-structure of suspended single-wall carbon nanotubes lying in two parallel planes separated by an inter-plane distance d (see Fig. 1). Nevertheless, some generic properties of QCB may be described under the assumption that QCB is a genuine $2D$ system. We choose coordinate system so that 1) the axes x_j and corresponding basic unit vectors $\mathbf{e}_j$ are oriented along the j-th array; 2) the x_3 axis is perpendicular to the QCB plane; 3) the x_3 coordinate is zero for the second array, and $-d$ for the first one. The basic vectors of the reciprocal superlattice for a square QCB are $Q\mathbf{e}_{1,2}$, $Q = 2\pi/a$ so that an arbitrary reciprocal superlattice vector $\mathbf{m}$ is a sum $\mathbf{m} = \mathbf{m}_1 + \mathbf{m}_2$, where $\mathbf{m}_j = m_j Q\mathbf{e}_j$, ($m_j$ integer). The first BZ is a square $|q_{1,2}| \leq Q/2$ (see Fig. 2).

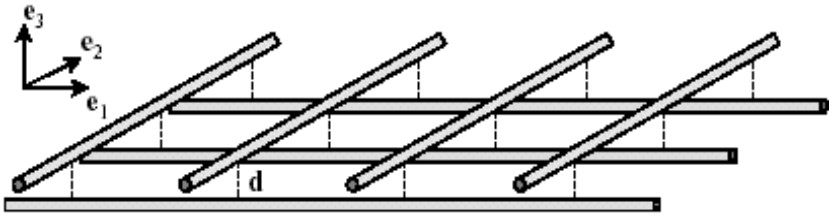

Figure 1: QCB. $\mathbf{e_j}$ - basic vectors of the coordinate system. Vector $\mathbf{e_1}$ ($\mathbf{e_2}$) is oriented along the first (second) array. The inter-array distance is d.

A single wire is characterized by its radius r_0, length L, and LL interaction parameter g. The minimal nanotube radius is $r_0 \approx 0.35$ nm [22], maximal nanotube length is $L \approx 1$ mm, and the LL parameter is estimated as $g \approx 0.3$ [13]. In typical experimental setup [6] the characteristic lengths mentioned above have the following values

$$d \approx 2 \text{ nm}, \quad L \approx 0.1 \text{ mm},$$

so that the inequalities

$$r_0 \ll d \ll a \ll L$$

are satisfied.

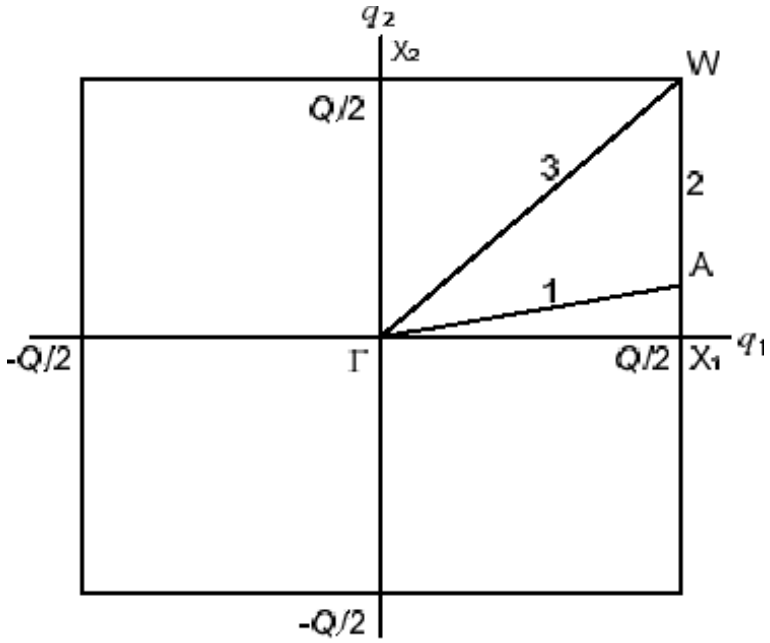

Figure 2: The first quarter of the BZ.

The QCB interaction H_E with an external electric field $\mathbf{E} = (E_1, E_2, E_3)$ is nothing but an energy of a set of QCB dipoles in this field

$$\begin{aligned} H_E &= -e\sqrt{2}\left\{\sum_{n_2}\int dx_1 E_1(x_1, n_2 a, -d)\theta_1(x_1, n_2 a, -d) + \right. \\ &\left. \sum_{n_1}\int dx_2 E_2(n_1 a, x_2, 0)\theta_2(n_1 a, x_2, 0),\right\} \end{aligned} \tag{1}$$

where θ_j is one of the two conventional canonically conjugate boson fields π_j, θ_j [19].

Before turning to investigation of QCB interaction with an external field, we briefly describe the spectral properties of the QCB itself [19]. We start with an isolated quantum wire of the j-th array. Its excitations are 1D LL

plasmons with wave numbers $q_j + m_j Q$ and frequencies $v|q_j + m_j Q|$. These plasmons can be treated in terms of "empty wire" excitations described by quasimomenta q_j, band number $s_j = 1 + [2\omega_{s_j}(q_j)/vQ]$ (square brackets denote integer part of a number), and dispersion law $\omega_{s_j}(q_j) = v|q_j + m_j Q|$. The direct products of such eigenstates of two arrays form the eigenstates of a $2D$ "empty lattice". They are characterized by quasimomenta $\mathbf{q} + \mathbf{m}$ and band number $s = 1 + [2(\omega_{s_1}(q_1) + \omega_{s_2}(q_2))/vQ]$.

Inter-array interaction turns "empty lattice" into QCB. In the actual region of QCB parameters, this interaction is very small. Hence it grossly conserves the unperturbed $1D$ systematics of levels and states, at least in the low energy region corresponding to the first few frequency bands. This means that perturbed eigenstates can be described in terms of the same quantum numbers (array number, band number and quasimomentum) as the plasmons of an "empty lattice". Such a description fails in two specific regions of the reciprocal space $\mathbf{k} = k_1\mathbf{e}_1 + k_2\mathbf{e}_2$. The first one is the vicinity of the high symmetry lines $k_j = nQ/2$ with n integer (the lines with $n = \pm 1$ include the BZ boundaries). Around these lines, the *inter-band* mixing is significant and two modes from adjacent bands are degenerate. The second region is the vicinity of the resonant lines $k_1 \pm k_2 = nQ$ where the eigenfrequencies of the unperturbed plasmons

$$\omega_j(\mathbf{k}) = v|k_j|, \quad j = 1, 2,$$

from the same band propagating along two arrays coincide $\omega_1(\mathbf{k}) = \omega_2(\mathbf{k} + \mathbf{m})$. The *inter-array* mixing is significant around the resonant lines where two modes corresponding to different arrays are degenerate. The inter-array interaction lifts these degeneracies and splits degenerate frequencies.

Thus, the inter-array interaction introduces real two dimensionality into the problem. Fig. 3 (see also Fig. 5 below) illustrates characteristic 2D features of the QCB spectrum. One can see well pronounced inter-array splitting around the BZ diagonal ΓW and inter-band splitting in the vicinity of the BZ corner W. The simplest way to probe $2D$ nature of QCB is to observe this splitting in the corresponding spectral region. Possible ways of such an observation are discussed in the next section.

3 Infrared absorption in QCB

3.1 Absorption in the BZ center

In the case of a dielectric substrate transparent in the infrared region, one can treat QCB as an isolated grid (without substrate) interacting directly

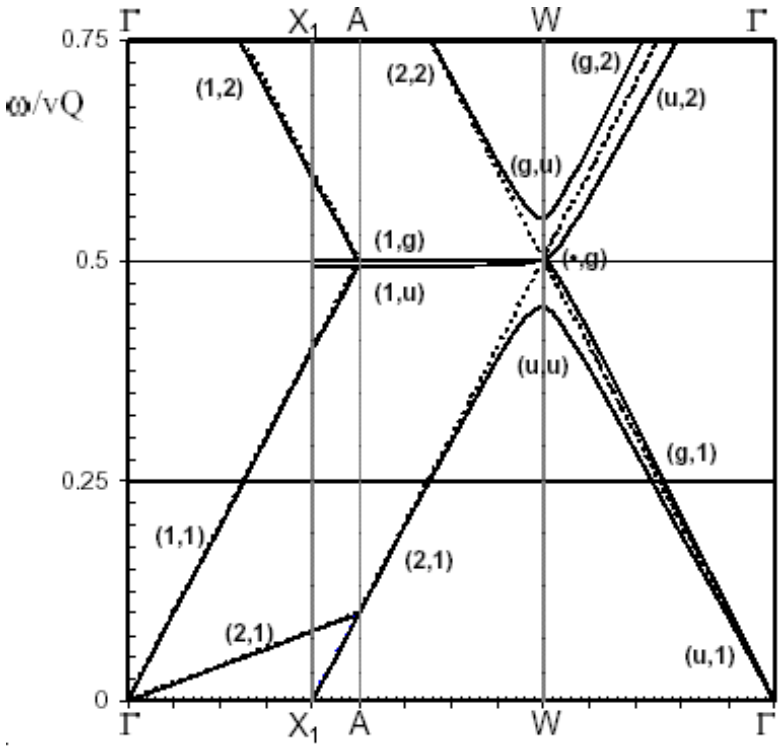

Figure 3: The energy spectrum of QCB (solid lines) and noninteracting arrays (dashed lines) along the lines ΓA, X_1W, and ΓW in Fig. 2.

with the incident radiation. Consider the simplest geometry (see Fig. 4 for details) where an external wave falls normally onto QCB plane, and its electrical field

$$\mathbf{E} = E_0 \mathbf{e}_1 \cos(\mathbf{kr} - \omega t)$$

is parallel to the lower (first) array. In this geometry the field $\mathbf{E}$ is *longitudinal* for array 1 and *transverse* for array 2 (see Fig. 4).

The eigenfrequencies of the transverse modes in array 2 substantially exceed the IR frequency of the incident wave and even the standard LL ultraviolet cutoff frequency. Thus, the incident wave can be treated as a static polarization field for this array, and the factor $\cos \omega t$ can be omitted. Then, the polarization waves in array 2 form a longitudinal diffraction field for array 1 with quasi wave vectors nQ (n integer). Further, the characteristic order of magnitude Q of a QCB plasmon wave vector is much larger than

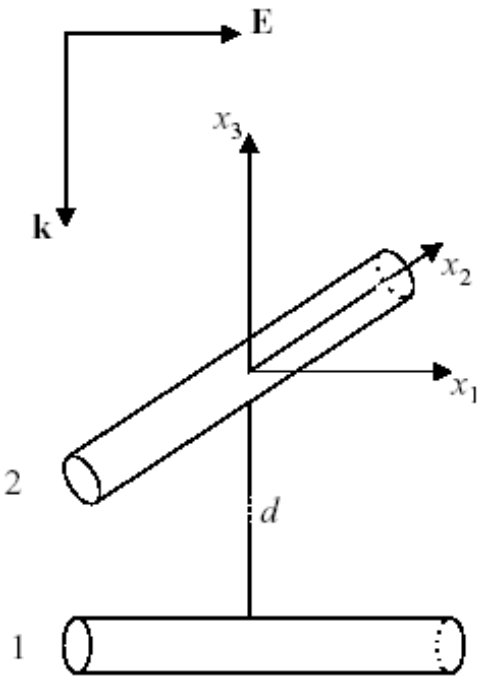

Figure 4: The incident field orientation with respect to QCB. The axes x_1 and x_2 are directed along the corresponding arrays, and d is the inter-array vertical distance (along the x_3 axis).

the wave vector $\mathbf{k}$ of the incident light, and we put the latter equal to zero from the very beginning. Then, the light wavelength is much larger than a nanotube diameter and the geometric shadow effect can be neglected. As a result the total field which affects array 1 consists of an external field and a diffraction field produced by a static charge induced in array 2.

To calculate a diffraction field consider first the field $\mathbf{E}^0$ produced by the quantum wire of array 2 which is located at $x_1 = x_3 = 0$ and labelled by $n_1 = 0$. The large distance between the wire under consideration and its neighbor partners from the same array allows one to neglect the influence of the charges induced on them. The static potential on the surface of the wire includes external potential of an incident field and the potential Φ^0 of the charge induced on the wire. On the other hand this static potential should be equal to a constant which we choose to be zero. In cylindrical coordinates

r, ϑ, x_2, $x_1 = r\cos\vartheta, x_3 = r\sin\vartheta$, this condition reads

$$\Phi^0(R_0, \vartheta, x_2) = E_0 r_0 \cos\vartheta. \tag{2}$$

Outside the wire, the induced potential Φ^0 satisfies Laplace equation $\Delta\Phi^0 = 0$. Solving this equation with boundary condition (2) we obtain the static part of the induced potential

$$\Phi^0(r, \vartheta, x_2) = \frac{E_0 r_0^2}{r}\cos\vartheta$$

and the corresponding static part of the induced field along the x_1 direction

$$E_1^0(x_1, x_3) = -E_0 \frac{r_0^2\left(x_3^2 - x_1^2\right)}{\left(x_3^2 + x_1^2\right)^2}.$$

The first component of the diffraction field is the sum of the fields induced by all wires of the upper array,

$$\begin{aligned} E_1(x_1; t) &= \cos\omega t \sum_{n_1} E_1^0(x_1 - n_1 a, -d) \\ &= -E_0 \cos\omega t \sum_{n_1} \frac{r_0^2\left(d^2 - (x_1 - n_1 a)^2\right)}{\left(d^2 + (x_1 - n_1 a)^2\right)^2}. \end{aligned} \tag{3}$$

This field is a periodic function of x_1 with period a. Therefore, its Fourier expansion contains only wave vectors $k_{1n} = nQ$ (n is the order of diffraction). This means that only frequencies $\omega_n = nvQ$ can be excited. In this case it is more convenient to expand the field over Bloch eigenfunctions of an "empty" wire [19]. These functions are labelled by quasimomentum q_1, $|q_1| \le Q/2$, and the band number s. The expansion includes only $q_1 = 0$ components and has the form

$$E_1(x_1; t) = \cos\omega t \sum_s E_{[s/2]} u_s(x_1),$$

where

$$u_s(x) = \exp\left(iQx[s/2](-1)^{s-1}\right)$$

is the $q_1 = 0^+$ Bloch amplitude $u_{sq_1}(x)$ within the s-th band, $[\dots]$ is the entire part symbol, and

$$E_n = -E_0 \frac{\pi r_0^2}{ad} nQd e^{-nQd}. \tag{4}$$

The excited eigenfrequency $\omega_n = \omega_{[s/2]}$ belongs simultaneously to the top of the lower even band with number $s = 2n$ and to the bottom of the upper odd band with number $s = 2n+1$ (this is the result of $\mathbf{E}(x)$ parity). Incident field corresponds to $n = 0$, and we do not take it into account.

Turning to the $\mathbf{q}, s$ representation with the help of the expansion

$$\theta_1(x_1, n_2 a) = \frac{\sqrt{a}}{L} \sum_{s\mathbf{q}} \theta_{1s\mathbf{q}} e^{i(q_1 x_1 + q_2 n_2 a)} \exp\left(iQx_1[s/2](-1)^{s-1}\mathrm{sign}q_1\right), \quad (5)$$

and similarly for θ_2 and $\pi_{1,2}$, one easily sees that only the $\mathbf{q} = \mathbf{0}$ components are involved in interaction with the incident radiation. The corresponding Hamiltonian has the form (zero quasimomentum index is omitted):

$$H_E = -\frac{eL}{\sqrt{2a}} \cos\omega t \sum_s E_{[s/2]} \left(\theta_{1s}^\dagger + \theta_{1s}\right),$$

Consider the initial frequency ω close to ω_n. In a resonant approximation, only four equations of motion for the "coordinate" operators θ_s with $s = 2n, 2n+1$ are relevant

$$\begin{aligned}
\ddot{\theta}_{1,2n} + \omega_n^2 \theta_{1,2n} + \phi\omega_n^2 (\theta_{2,2n} - \theta_{2,2n+1}) &= L f_n \cos\omega t, \\
\ddot{\theta}_{1,2n+1} + \omega_n^2 \theta_{1,2n+1} - \phi\omega_n^2 (\theta_{2,2n} - \theta_{2,2n+1}) &= L f_n \cos\omega t, \\
\ddot{\theta}_{2,2n} + \omega_n^2 \theta_{2,2n} + \phi\omega_n^2 (\theta_{1,2n} - \theta_{1,2n+1}) &= 0, \\
\ddot{\theta}_{2,2n+1} + \omega_n^2 \theta_{2,2n+1} - \phi\omega_n^2 (\theta_{1,2n} - \theta_{1,2n+1}) &= 0, \qquad (6)
\end{aligned}$$

where

$$f_n = \frac{\sqrt{2} vge}{\hbar\sqrt{a}} E_n$$

and the main small parameter of the problem

$$\phi = 2\frac{ge^2}{\hbar v}\frac{r_0^2}{ad} \approx 0.007$$

is the dimensionless inter-array interaction. The homogeneous part of the system (6) defines four eigenfrequencies,

$$\begin{aligned}
\omega_{gg} &= \omega_{ug} = \omega_n, \\
\omega_{uu} &\approx \omega_n(1-\phi), \\
\omega_{gu} &\approx \omega_n(1+\phi).
\end{aligned}$$

The corresponding eigenvectors are symmetrized combinations of the four operators which enter Eq. (6). They have a fixed parity with respect to

permutation of arrays (the first index) and neighboring bands (the second index). Only the following two modes (even with respect to band index)

$$\theta_{gg} = \frac{1}{2}\left(\theta_{1,2n} + \theta_{1,2n+1} + \theta_{2,2n} + \theta_{2,2n+1}\right),$$
$$\theta_{ug} = \frac{1}{2}\left(\theta_{1,2n} + \theta_{1,2n+1} - \theta_{2,2n} - \theta_{2,2n+1}\right)$$

interact with an external field. Therefore only the unperturbed frequency $\omega_n = \omega_{gg} = \omega_{ug}$ will be absorbed. The two equations of motion for the operators $\theta_{gg,ug}$ have the same form

$$\ddot{\theta}_\alpha + 2\gamma\dot{\theta}_\alpha + \omega_n^2\theta_\alpha = Lf_n \cos\omega t,$$

where $\alpha = gg, ug$ and γ is an attenuation coefficient introduced phenomenologically. Employing standard procedure in the vicinity of the resonance $|\omega - \omega_n| \ll \omega_n$ immediately yields the relative absorption of Lorentz type

$$\frac{\Delta I_n}{I_0} = 2g\frac{e^2}{\hbar c}\left(\frac{\pi r_0^2}{ad}\right)^2 \frac{\gamma v Q}{(\omega - \omega_n)^2 + \gamma^2}\left[nQde^{-nQd}\right]^2, \tag{7}$$

where

$$I_0 = \frac{cL^2}{4\pi}E_0^2$$

is the energy of light that falls on the QCB per unit time.

Due to the exponential term in the r.h.s of Eq. (4), E_n decreases quickly with n and only the first few terms contribute to absorption. The characteristic dimensionless scale of the induced field $r_0^2/(ad)$ for typical values of QCB parameters equals 0.004. In Fig. 5 we plot the lowest part of absorption spectrum. The figure shows that one can probe at least the first five spectral lines corresponding to ω_n with $n = 1, 2, \ldots, 5$.

The width of the absorption line (7) is governed by an attenuation coefficient γ. We expect its value to be small. Indeed, the attenuation is caused mainly by decay of plasmon into phonons. The one phonon decay of the plasmon with wave number k and frequency $\omega = v|k|$ into a single phonon with the same ω and k occurs in a single point in $1D$ and does not yield finite attenuation at all. Multi-phonon decay is weak because of the small anharmonic coupling within the wire. As a result, the form of the absorption lines should be determined mainly by the instrumental linewidth.

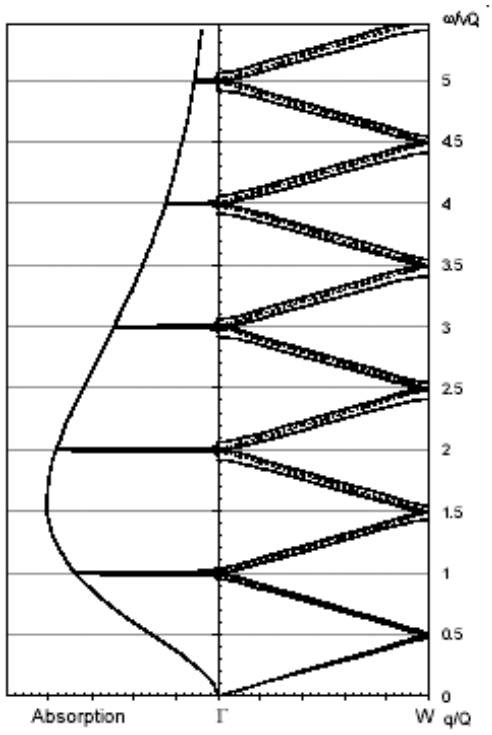

Figure 5: The lowest ten bands of the QCB spectrum along the BZ diagonal ΓW and the corresponding single lines of direct IR absorption.

3.2 Scanning of the spectrum

Within a geometry considered in the previous subsection, one can probe plasmon spectrum only at the BZ center. To study plasmons with nonzero wave vectors one should add to the system an external diffraction lattice namely a periodic array of metallic stripes parallel to the Y axis (see Fig. 6). The DL plane $Z = 0$ is parallel to the QCB planes $Z = -D$ for the upper second array and $Z = -(D + d)$ for the lower first array (the Z axis is parallel to the x_3 axis). The distance D between DL and second array is of the same order as the inter-array distance $d = 2$ nm. The angle between DL wires and the *second* array is φ $(0 < \varphi < \pi/2)$. To get a wave number K of a diffraction field much smaller than Q one needs a DL with a period A much larger than the QCB period a. In the following numerical estimations we choose $A \approx 100$ nm.

Consider an incident field with electric vector $\mathbf{E} = E_0 \mathbf{e}_X \cos(\mathbf{kr} - \omega t)$

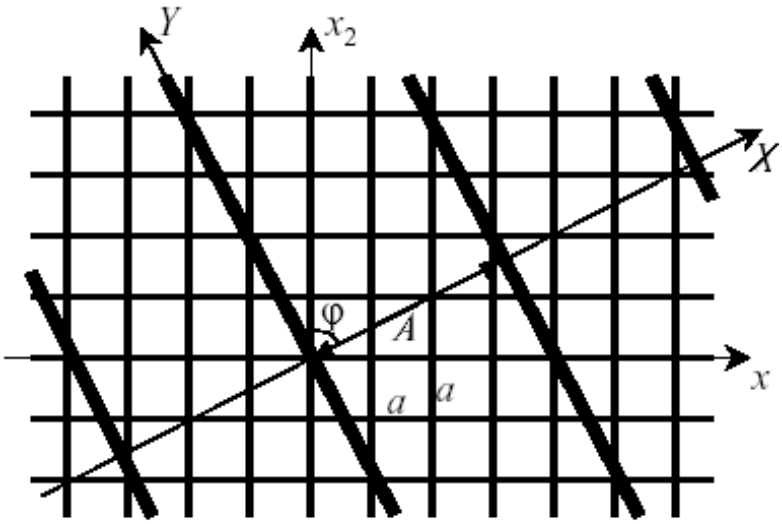

Figure 6: QCB and DL. The X, Y axes are oriented along the DL stripes and the wave vector $\mathbf{K}$ of the diffraction field respectively. The DL (QCB) period is A (a).

oriented along the X axis (perpendicular to the DL wires). The radius R_0 of a DL wire is assumed to be not much larger than the nanotube radius r_0. In this case light scattering on the DL is similar to that considered in Subsection 3.1. Then the diffraction field is concentrated along the X direction and has the form (compare with Eq. (3))

$$E_X(X, Z, t) = -E_0 \cos \omega t \sum_N \frac{R_0^2(Z^2 - (X - NA)^2)}{(Z^2 + (X - NA)^2}.$$

The Fourier transform of the diffraction field is

$$E_X(\mathbf{K}, Z) = -E_0 \frac{\pi R_0^2}{A|Z|} |KZ| e^{-|KZ|}, \tag{8}$$

where

$$\mathbf{K}(M) = K\mathbf{e}_X = (K_1, K_2) = \frac{2\pi M}{A}(\sin\varphi, \cos\varphi)$$

with positive integer M. This means that all the points $\mathbf{K}$ lie on the same ray oriented along the positive direction of the X axis. The vector $\mathbf{K}(M)$

for a fixed M can be uniquely represented as a sum of quasimomenta lying in the first BZ and two reciprocal lattice vectors

$$\mathbf{K}(M) = \mathbf{q}(M) + \mathbf{m}_1(M) + \mathbf{m}_2(M).$$

The field components

$$\begin{aligned} E_{1\mathbf{K}} &= E_X(\mathbf{K}, D+d)\sin\varphi, \\ E_{2\mathbf{K}} &= E_X(\mathbf{K}, D)\cos\varphi \end{aligned} \tag{9}$$

parallel to the quantum wires can excite plasmons and contribute to the absorption process.

The Hamiltonian (1) of QCB interacting with an external field in Fourier representation reads,

$$H_E = \frac{\hbar L}{2vg}\sum_{j\mathbf{K}} f_{j,\mathbf{K}}\left(\theta_{j,\mathbf{K}} + \theta^{\dagger}_{j,\mathbf{K}}\right),$$

where

$$f_{j,\mathbf{K}} = \frac{\sqrt{2}vge}{\hbar\sqrt{a}}E_{j,\mathbf{K}}, \qquad \mathbf{m} = \mathbf{m}_1 + \mathbf{m}_2.$$

The equations of motion for boson fields have the form

$$\begin{aligned} \ddot{\theta}_{1,\mathbf{q}+\mathbf{m}_1} + \omega^2_{q_1+m_1Q}\theta_{1,\mathbf{q}+\mathbf{m}_1} + 2\gamma\dot{\theta}_{1,\mathbf{q}+\mathbf{m}_1} &+ \\ + \sum_{m_2}\Phi_{\mathbf{q}+\mathbf{m}}\theta_{2,\mathbf{q}+\mathbf{m}_2} &= L\sum_{M,m_2} f_{1,\mathbf{K}}\delta_{\mathbf{K},\mathbf{q}+\mathbf{m}}, \\ \ddot{\theta}_{2,\mathbf{q}+\mathbf{m}_2} + \omega^2_{q_2+m_2Q}\theta_{2,\mathbf{q}+\mathbf{m}_2} + 2\gamma\dot{\theta}_{1,\mathbf{q}+\mathbf{m}_1} &+ \\ + \sum_{m_1}\Phi_{\mathbf{q}+\mathbf{m}}\theta_{1,\mathbf{q}+\mathbf{m}_1} &= L\sum_{M,m_1} f_{2,\mathbf{K}}\delta_{\mathbf{K},\mathbf{q}+\mathbf{m}}, \end{aligned} \tag{10}$$

where

$$\Phi_{\mathbf{k}} = \phi\xi_{k_1}\xi_{k_2}, \;\; \xi_k = \omega_k \mathrm{sign}k, \;\; \omega_k = v|k|,$$

and γ is the same phenomenological attenuation coefficient as in Subsection 3.1. Only the first few modes in the sum over K in the r.h.s. of Eq. (10) effectively excite the QCB plasmons. Indeed, the diffraction field (8) is proportional to the same dimensionless function of the type te^{-t} ($t = KZ_j$) as in the previous subsection (see Eq. (4)). This function has its maximum at $t = 1$ and differs significantly from zero for $0.2 < t < 2.7$. For $a = 20$ nm,

$D = 2$ nm, it is of order unity within the interval $0.18Q < K < 2.13Q$ for the first array ($Z_1 = D + d$), and within the interval $0.36Q < K < 4.26Q$ for the second array ($Z_1 = D$). This means that one can excite the modes of the four lower bands ($K < 2Q$) of the first array and the modes of eighth lower bands ($K < 4Q$) of the second array.

According to Eqs. (9) the field $E_{j\mathbf{K}(M)}$ is coupled with plasmons of wave vectors $\mathbf{q} + \mathbf{m}_j = \mathbf{q}(M) + \mathbf{m}_j(M)$ within the j-th array. The nature of the excited plasmons as well as their frequencies depend on the direction of the vector $\mathbf{K}(M)$. For simplicity we restrict ourselves by acute angles $0 < \varphi < \pi/2$ describing orientation of both DL and vector $\mathbf{K}(M)$. There are four kinds of dimensional crossover depending on specific directions in the BZ. Each type of crossover is characterized by its own set of absorption lines. The first one takes place in a common case when $\mathbf{K}(M)$ for any M never reaches neither a resonant direction nor the BZ boundary. The second case corresponds to the bisectorial direction $\varphi = \pi/4$ where the main resonant condition $\omega(K_1) = \omega(K_2)$ is fulfilled. The third group of directions is determined by another resonant condition $\omega(K_1) = \omega(nQ \mp K_2)$. Finally, the fourth group is formed by directions intersecting with the BZ boundaries for some values of M. In what follows we consider these four cases separately.

1. In the general case, the points $\mathbf{K}(M)$ for all M are far from the BZ diagonals and boundaries. Therefore each of them corresponds to two plasmons mostly propagating along the j-th array, $j = 1, 2$, with unperturbed frequencies $\omega_{K_j(M)} = vK_j(M)$. The inter-array interaction slightly renormalizes the eigenfrequencies

$$\begin{aligned}
\omega^2_{1\mathbf{K}} &= \omega^2_{K_1} + \phi^2 \sum_{m_2} \frac{\omega^2_{K_1}\omega^2_{K_2+m_2Q}}{\omega^2_{K_1} - \omega^2_{K_2+m_2Q}}, \\
\omega^2_{2\mathbf{K}} &= \omega^2_{K_2} + \phi^2 \sum_{m_1} \frac{\omega^2_{K_2}\omega^2_{K_1+m_1Q}}{\omega^2_{K_2} - \omega^2_{K_1+m_1Q}}.
\end{aligned}$$

Thus, increasing the frequency of an incident light one observes a set of single absorption lines that consists of two almost equidistant subsets with frequencies corresponding to excitation of plasmons in the first or second arrays. The distances between adjacent lines within each subset are

$$\begin{aligned}
\Delta\omega_1 &= v\Delta K_1 = 2\pi v \sin\varphi/A, \\
\Delta\omega_2 &= v\Delta K_2 = 2\pi v \cos\varphi/A,
\end{aligned}$$

and their ratio depends on the DL orientation φ only

$$\frac{\Delta\omega_1}{\Delta\omega_2} = \tan\varphi.$$

The equations of motion for the "coordinate" operators $\omega_{1\mathbf{K}}$ and $\omega_{2\mathbf{K}}$ can be written in the resonant approximation as:

$$\ddot{\theta}_{j\mathbf{K}} + \omega^2_{j\mathbf{K}}\theta_{j\mathbf{K}} + 2\gamma\dot{\theta}_{j\mathbf{K}} \;=\; f_{j\mathbf{K}}, \qquad j = 1, 2.$$

The relative absorption is of the Lorentz type

$$\begin{aligned}
\frac{\Delta I_{1\mathbf{K}}}{I_0} &= 2g\frac{e^2}{\hbar c}\left(\frac{\pi R_0^2}{AD}\right)^2 \frac{\gamma v Q}{\left(\omega-\omega_{1\mathbf{K}}\right)^2+\gamma^2}\left(KDe^{-KD}\cos\varphi\right)^2, \\
\frac{\Delta I_{2\mathbf{K}}}{I_0} &= 2g\frac{e^2}{\hbar c}\left(\frac{\pi R_0^2}{AD}\right)^2 \frac{\gamma v Q}{\left(\omega-\omega_{2\mathbf{K}}\right)^2+\gamma^2}\left(KDe^{-K(D+d)}\sin\varphi\right)^2. \qquad (11)
\end{aligned}$$

2. In the resonant case $\varphi = \pi/4$, the condition $K_1(M) = K_2(M)$ is satisfied for all M. Therefore modes propagating along the two arrays are always degenerate. Inter-array interaction lifts the degeneracy. Indeed, in the resonant approximation, the coupled equations of motion for the field operators read

$$\begin{aligned}
\ddot{\theta}_{1\mathbf{K}} + \omega^2_{K_1}\theta_{1\mathbf{K}} + \phi\omega^2_{K_1}\theta_{2\mathbf{K}} + 2\gamma\dot{\theta}_{1\mathbf{K}} &= f_{1\mathbf{K}}, \\
\ddot{\theta}_{2\mathbf{K}} + \omega^2_{K_1}\theta_{2\mathbf{K}} + \phi\omega^2_{K_1}\theta_{1\mathbf{K}} + 2\gamma\dot{\theta}_{2\mathbf{K}} &= f_{2\mathbf{K}}.
\end{aligned}$$

After symmetrization $\theta_{g,u} = (\theta_{1\mathbf{K}} \pm \theta_{2\mathbf{K}})/\sqrt{2}$, they have the same form

$$\ddot{\theta}_{\alpha\mathbf{K}} + \omega^2_{\alpha,K_1}\theta_{\alpha\mathbf{K}} + 2\gamma\dot{\theta}_{\alpha\mathbf{K}} = f_{\alpha,\mathbf{K}}, \quad \alpha = g, u,$$

where

$$\omega_{g/u,K_1} = \omega_{K_1}\left(1 \pm \frac{1}{2}\phi\right)$$

are the renormalized frequencies and

$$f_{g/u,\mathbf{K}} = (f_{1\mathbf{K}} \pm f_{2\mathbf{K}})/\sqrt{2}.$$

The amplitudes $f_{\alpha\mathbf{K}}$ are of the same order of magnitude because the distances D and d have the same order of magnitude. As a result, increasing

the frequency of an incident light one observes an equidistant set of absorption doublets with distance $\pi\sqrt{2}v/A$ between adjacent doublets (see Fig. 7). The relative absorption is of the Lorentz type

$$\frac{\Delta I_{g/u,\mathbf{K}}}{I_0} = \frac{g}{2}\frac{e^2}{\hbar c}\left(\frac{\pi R_0^2}{AD}\right)^2 \frac{\gamma v Q}{\left(\omega - \omega_{g/u,K_1}\right)^2 + \gamma^2}\left[KD\left(e^{-KD} \pm e^{-K(D+d)}\right)\right]^2. \tag{12}$$

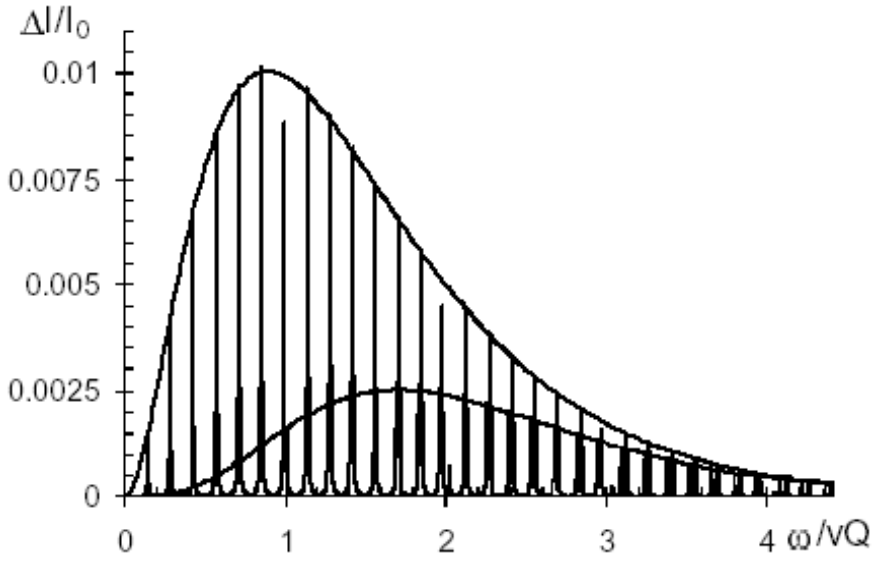

Figure 7: Absorption doublets (isolated peaks) in the resonant direction $\varphi = \pi/4$. Two envelopes corresponding to two components of each doublet are rather distingiushable.

3. Consider now the directions φ determined by the equation

$$\sin\left(\varphi \pm \frac{\pi}{4}\right) = \frac{nA}{\sqrt{2}M_0 a}, \tag{13}$$

where n and M_0 are mutually prime integers. For this direction, two components of the first $M_0 - 1$ points $\mathbf{K}(M)$ do not satisfy any resonant condition while the M_0-th one does

$$K_1(M_0) \pm K_2(M_0) = nQ. \tag{14}$$

With increasing M this situation is reproduced periodically so that all points $\mathbf{K}(pM_0)$ with p integer satisfy a similar condition with pn standing instead of n, while all intermediate points are out of resonance.

In the zero approximation with respect to the inter-array interaction we expect appearance of two sets of absorption lines with frequencies $p\omega_j = vK_j(pM_0)$, $j = 1, 2$, corresponding to excitation of plasmons within the $pm_j(M_0)$-th band of the j-th array. The ratio of the frequencies ω_j is defined by DL orientation

$$\frac{\omega_1}{\omega_2} = \tan\varphi.$$

The relative absorption for these lines is described by Eqs.(11). However, due to the resonance condition (14), a plasmon in the first array with the wave vector $\mathbf{K} = (K_1(pM_0), K_2(pM_0))$ and frequency $\omega_1 = vK_1(pM_0)$ is coupled with a plasmon in the second array with the same frequency and the wave vector $\mathbf{K'} = (K_2(pM_0), K_1(pM_0))$ (inter-array degeneracy). Similarly, a plasmon in the second array with the wave vector $\mathbf{K} = (K_1(pM_0), K_2(pM_0))$ and frequency $\omega_2 = vK_2(pM_0)$ is coupled with a plasmon in the first array with the same frequency and the wave vector $\mathbf{K'} = (K_2(pM_0), K_1(pM_0))$. This degeneracy of two modes corresponding to the same band but to different arrays is lifted by the inter-array interaction. As a result one has two sets of doublets instead of two sets of single lines. In the resonant approximation, the coupled equations of motion for the field operators read

$$\begin{aligned} \ddot{\theta}_{1\mathbf{K}} + \omega_{K_1}^2\theta_{1\mathbf{K}} + \phi\omega_{K_1}^2\theta_{2\mathbf{K'}} + 2\gamma\dot{\theta}_{1\mathbf{K}} &= f_{1\mathbf{K}}, \\ \ddot{\theta}_{2\mathbf{K'}} + \omega_{K_1}^2\theta_{2\mathbf{K'}} + \phi\omega_{K_1}^2\theta_{1\mathbf{K}} + 2\gamma\dot{\theta}_{2\mathbf{K'}} &= 0, \end{aligned} \qquad (15)$$

where $\mathbf{K} = (K_1, K_2)$, $\mathbf{K'} = (K_2, K_1)$, K_1 and K_2 satisfy the resonance condition (14). The similar equations take place for the operators $\theta_{1\mathbf{K'}}$ and $\theta_{2\mathbf{K}}$. After symmetrization $\theta_{g,u} = (\theta_{1\mathbf{K}} \pm \theta_{2\mathbf{K'}})/\sqrt{2}$, they have the same form

$$\ddot{\theta}_\alpha + \omega_{\alpha K_1}^2\theta_\alpha + 2\gamma\dot{\theta}_\alpha = \frac{1}{\sqrt{2}} f_{1\mathbf{K}}.$$

The relative absorption is of the Lorentz type

$$\frac{\Delta I_{g/u,\mathbf{K}}}{I_0} = g\frac{e^2}{\hbar c}\left(\frac{\pi R_0^2}{AD}\right)^2 \frac{\gamma v Q}{\left(\omega - \omega_{g/u,K_1}\right)^2 + \gamma^2}\left(KDe^{-KD}\cos\varphi\right)^2. \qquad (16)$$

The relative absorption for the second doublet is obtained from Eq. (16) after permutation $K_1 \to K_2$ and replacement $D \to D + d$ in the exponent expression.

Thus, for such orientation of DL, when increasing the frequency of an incident wave one should observe two equidistant sets of single absorption lines with two sets of equidistant doublets built in these series

$$\omega_{1\mathbf{K}} = \omega_{K_1(pM_0)}\left(1 \pm \frac{1}{2}\phi\right),$$
$$\omega_{2\mathbf{K}} = \omega_{K_2(pM_0)}\left(1 \pm \frac{1}{2}\phi\right).$$

Consider the case $n = 1$ and $A/a = 5$, which corresponds to the realistic values of the parameters $a = 20$ nm and $A = 100$ nm. Here the first angle that satisfies Eq. (13) appears at $M_0 = 4$ and equals $\varphi_1 \approx 17°07'$. Two lowest doublets of each sequence of doublets correspond to $p = 1$ and are centered around the frequencies $4\omega_1 = 0.76vQ$ and $4\omega_2 = 0.24vQ$. The lower of them lies within the first energy band, whereas the upper one lies in the second band. The singlet absorption lines generated by the frequency ω_1 and one series of the doublets corresponding to frequencies multiple integer to $4\omega_1$ are displayed in Fig. 8. Surprisingly, one can see an additional doublet opening additional series of doublets with frequencies $15\omega_1$. The reason is that the chosen direction φ_1 is very close to another one higher resonance direction $\varphi_2 \approx 16°52'$ satisfying to Eq. (13) with $M_0 = 15$, $n = -2$, and the sign "minus" in the l.h.s..

4. It seems that a similar behavior should be observed in the case when the points $\mathbf{K}_{pM}$ lie at one of the BZ boundaries, i.e. satisfy the relation

$$K_j(pM_j) = \frac{npQ}{2}$$

with some specific values j, M_j and n. Such situation is realized at specific angles that depend on the integers j, n, M_j. In the vicinity of the points $\mathbf{K}(pM_j)$ two frequencies corresponding to the unperturbed modes of the j-th array from the np-th and $(np+1)$-th bands coincide. This is the case of inter-band degeneracy that is also lifted by inter-array interaction. Due to the square symmetry (invariance with respect to $x_j \to -x_j$ inversion), only one of the two components with frequency $\omega = v|K_j(pM_j)|$ may be excited by a diffraction field. Therefore, this case does not differ from the case **1** considered above and two sets of equidistant single lines can be observed.

We emphasize that studying absorption of light by QCB one can expose not only the known [19] dimensional crossover with respect to an angle (direction), but also occurrence of a new type of crossover with *an external*

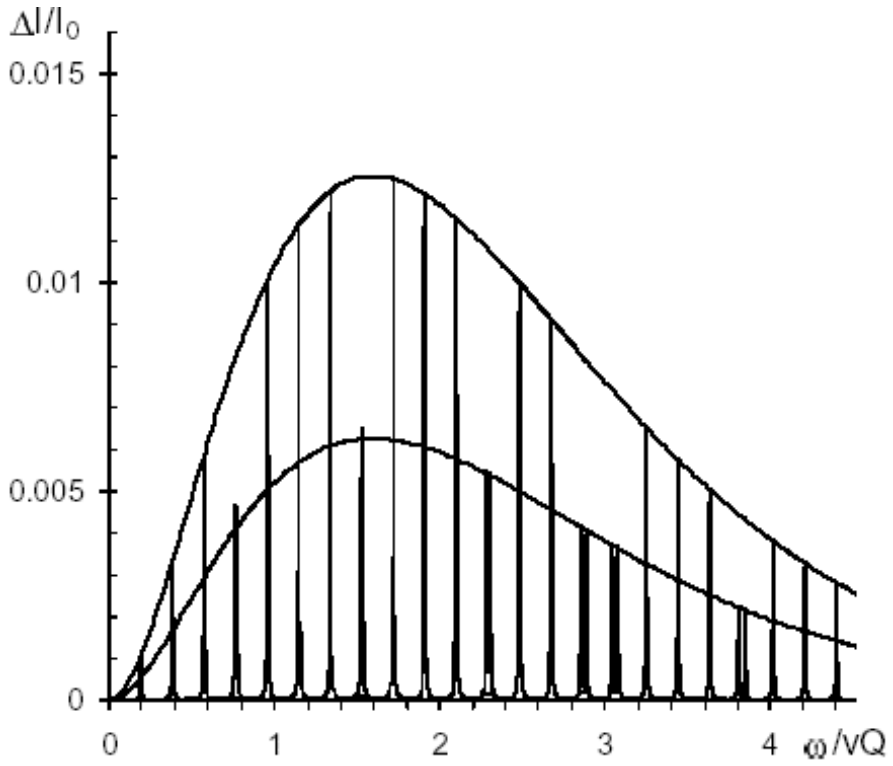

Figure 8: Absorption spectrum in a higher resonance direction $\varphi \approx 17^\circ$ contains two sets of doublets with periods $4\omega_1$ and $15\omega_1$.

frequency as a control parameter. This occurs for special directions of type **3** where, with increasing frequency, the set of single lines is periodically intermitted by doublets.

4 Conclusion

In conclusion, we have investigated the possibility of spectroscopic studies of the excitation spectrum of quantum crossbars, which possesses unique property of dimensional crossover both in spatial coordinates and in the $(\mathbf{q}, \omega)$ coordinates. It follows from our studies that the plasmon excitations in QCB may be involved in resonance diffraction of incident electromagnetic waves and in optical absorption in the IR part of the spectrum. This absorption strongly depends on the direction of the wave vector $\mathbf{q}$. One can

observe dimensional crossover from $1D$ to $2D$ behavior of QCB by scanning an incident angle. The crossover manifests itself in the appearance of a set of absorption doublets instead of the set of single lines. At special directions, one can observe new type of crossover where doublets replace the single lines with changing frequency at a fixed $\mathbf{q}$ direction.

Numerous helpful discussions with K. Kikoin, and Y. Avishai are greatly appreciated.

References

[1] J.E. Avron, A. Raveh, and B. Zur, Rev. Mod. Phys. **60**, 873 (1988).

[2] Y. Avishai and J.M. Luck, Phys. Rev. B **45**, 1074 (1992).

[3] F. Guinea and G. Zimanyi, Phys. Rev. B **47**, 501 (1993).

[4] N.A. Melosh, A. Boukai, F. Dlana, B. Gerardot, A. Badolato, P.M. Petroff, and J.R. Heath, Science **300**, 112 (2003).

[5] Y. Luo, C.P. Collier, J.O. Jeppesen, K.A. Nielsen, E. Delonno, G. Ho, J. Perkins, H-R. Tseng, T. Yamamoto, J.F. Stoddardt, and J.R. Heath, ChemPhysChem **3**, 519 (2002).

[6] T. Rueckes, K. Kim, E. Joselevich, G.Y. Tseng, C.L. Cheung, and C.M. Lieber, Science **289**, 94 (2000).

[7] R. Mukhopadhyay, C.L. Kane, and T.C. Lubensky, Phys. Rev. B **63**, 081103(R) (2001).

[8] A.B. Dalton, S. Collins, E. Muñoz, J.M. Razal, V.H. Ebron, J.P. Ferraris, J.N. Coleman, B.G. Kim, and R.H. Baughman, Nature **423**, 703 (2003).

[9] J.R. Heath and M.A. Ratner, Physics Today **March**, 43 (2003).

[10] J.M. Tranquada, J. Physique IV **12**, 239 (2002).

[11] G.V. Tseng, J.C. Ellenbogen, Science **294**, 1293 (2001).

[12] M. Bockrath, D.H. Cobden, J. Lu, A.G. Rinzler, R.E. Smalley, L. Balents, and P.L. McEuen, Nature **397**, 598 (1999).

[13] R. Egger, A. Bachtold, M.S. Fuhrer, M. Bockrath, D.H. Cobden, and P.L. McEuen, in: *Interacting Electrons in Nanostructures*, p. 125, Eds. R. Haug, and H. Schoeller (Springer, Berlin, 2001).

[14] X.G. Wen, Phys. Rev. B **42**, 6623 (1990).

[15] H.J. Schultz, Int. J. Mod. Phys. **1/2**, 57 (1991).

[16] I. Kuzmenko, S. Gredeskul, K. Kikoin, and Y. Avishai, Low Temp. Phys. **28**, 539 (2002) [Fiz. Nizk. Temp. **28**, 752 (2002)].

[17] A.H. Castro Neto and F. Guinea, Phys. Rev. Lett. **80**, 4040 (1998).

[18] R. Mukhopadhyay, C.L. Kane, and T.C. Lubensky, Phys. Rev. B **64**, 045120 (2001).

[19] I. Kuzmenko, S. Gredeskul, K. Kikoin, and Y. Avishai, Phys. Rev. B **67**, 115331 (2003).

[20] K. Kikoin, I. Kuzmenko, S. Gredeskul, and Y. Avishai, in: *Recent Trends in Theory of Physical Phenomena in High Magnetic Fields*. Eds. I.D. Vagner, T. Maniv, and P. Wyder, NATO Sci. Series, **106**, 89 (2003).

[21] S. Gredeskul, I. Kuzmenko, K. Kikoin, and Y. Avishai, Physica E **17**, 187 (2003).

[22] S.G. Louie, in: *Carbon Nanotubes*, Eds. M.S. Dresselhaus, G. Dresselhaus, and Ph. Avouris, Topics Appl. Phys. **80**, 113 (2001), (Springer, Berlin, 2001).